Catalysis Letters 53 (1998) 15–21

The structure and surface acidity of zirconia-supported tungsten oxides

Weijie Ji *, Jingqiu Hu and Yi Chen

School of Chemistry and Chemical Engineering, Nanjing University, Nanjing 210093, PR China

Received 4 March 1998; accepted 6 May 1998

The structure and surface acidity of zirconia-supported tungsten oxide are studied by using BET, XRD, FT Raman, Tian–Calvet microcalorimetry as well as XPS. Three different crystal forms of ZrO_2 and their hydroxide precursors were prepared in a controllable way. It was found that the starting material and preparing conditions used have a significant effect on the structure of ZrO_2 obtained. The tungstate species on zirconium hydroxide generally promote the transformation of the hydroxide precursor into tetragonal ZrO_2, while the same species on the pre-calcined ZrO_2 has less effect during calcination. A bulk-phase WO_3 existed in the samples prepared by initially impregnating the monoclinic, tetragonal and cubic ZrO_2 or the hydroxide precursors of m- and t-ZrO_2, while no crystalline WO_3 was present in the samples prepared by initially impregnating the hydroxide precursor of c-ZrO_2. Raman results revealed that the surface tungstate(s) on three different zirconium hydroxides or their respective zirconia have similar structural features before calcination. The surface tungsten oxides and some WO_3 bulk phase are the detectable tungsten species in the final samples, the ratio of each component is strongly dependent on the preparation history and the nature of the support. Creation of very strong acidic sites on the zirconia-supported tungsten oxide is related to the crystal form of zirconia itself, the type of tungsten oxide species, and the cooperation between the surface tungsten oxide overlayer and zirconia. The strong acidic sites can be completely poisoned by the remaining sodium ion impurities, but have not been appreciably influenced by added yttrium component. The crystalline WO_3 seems of little importance in building up the strong surface acidity.

Keywords: structure, surface acidity, tungsten oxide, zirconia

1. Introduction

Solid acids have wide applications in the catalysis field and belong to the group of new catalytic materials which are greatly developed in recent years [1,2]. There are advantages of using solid acids: (1) easy separation of the products, (2) less corrosion, less pollution and more environmentally friendly as compared with aqueous acids, (3) some solid acids, namely the solid superacids, can perform catalytic reactions at much lower temperature than that used in the traditional catalytic processes. On the other hand, there are still some difficulties in practical application of the solid acids; the major problems are in two aspects: (1) the strength of acidity of solid acids is generally not uniform, and (2) strong acidic sites are not durable and deactivate quickly.

Very strong solid acids include those zirconia-based materials which contain SO_4^{2-} species [3,4]. It was reported that specially prepared WO_3/ZrO_2 can show very strong acidity [5,6]. The authors emphasized that the strong acidic sites are related to the presence of tetragonal type ZrO_2, but the details for the creation of surface acidity still remain unclear.

So the main proposes for this study are as follows: (1) According to the literature, the certain form of ZrO_2 and its hydroxide precursor can be prepared via a controllable preparation procedure [7–10], thus the structure of zirconium oxide can be determined and the surface state of tungsten species on either zirconium oxide or its hydroxide precursor can be examined before and after calcination. (2) By microcalorimetry measurement of a basic probe molecule such as ammonia, the surface acidity of the zirconia-based samples can be quantitatively determined, therefore, the relationship might be established between the surface acidity and the crystal form of zirconia and the structural feature of surface tungsten species.

2. Experimental

2.1. Preparation of different forms of zirconia and their hydroxide precursors

Three methods are used to prepare different forms of zirconia and their hydroxide precursors. Methods A–C are adopted for preparing m-ZrO_2, t-ZrO_2, c-ZrO_2 and their hydroxide precursors, respectively. For method A, concentrated aqueous $NH_3{\cdot}H_2O$ was quickly added into 250 ml 0.4 M aqueous $ZrCl_4$ or $ZrOCl_2$ solution under stirring to obtain a suspension of zirconium hydroxide. After stirring 20 min and aging 2 h at room temperature, the suspension was filtrated and the paste was washed with distilled water until no Cl^- could be detected in the solution by using 0.1 M aqueous $AgNO_3$. Then the precipitate was dried at 378 K for 10 h and ground into powder for use. For method B, the procedure is basically the same

---

[*] To whom correspondence should be addressed.

as in method A, except that addition of $NH_3 \cdot H_2O$ is dropwise instead. After the suspension was formed, 250 ml 4.5 M NaOH solution was added under stirring for 20 min, then the suspension was aged for 4 h. After that, decantation of suspension and washing with 500 ml distilled water were performed under rigorous stirring for several times. Filtration and washing of the precipitate were operated (more than twenty-four times) until the pH of solution was around 7 and no Cl^- could be detected by using 0.1 M aqueous $AgNO_3$. Finally, the precipitate was dried at 378 K for 10 h. For method C, the same procedure was adopted as in method A, but using a mixture solution of $ZrCl_4$ and $Y(NO_3)_3$ in which the mole ratio of ZrO_2 to Y_2O_3 is 94 : 6. All the zirconium hydroxides prepared by the three methods mentioned above are calcined in air at 773 K for 4 h to obtain the corresponding ZrO_2.

2.2. Preparation of supported tungsten oxides

The samples were prepared by wetness impregnation. The zirconium hydroxide or zirconia powder was added into the aqueous solution of $(NH_4)_2WO_4$ (chemical pure, Shanghai Second Chemical Company) with the proper concentration under stirring at 333 K. The WO_3 content is 14 wt% [11]. After impregnation, the samples were dried in air at 383 K for 12 h and calcined at 973 K for 2 h, respectively.

2.3. Characterization

BET surface areas of the samples were measured by N_2 adsorption at 77 K. XRD measurements were performed on a Rigaku/D/Max-RA diffractometer with Cu Kα radiation. Laser Raman spectra in the 100–1200 cm^{-1} range were taken on a Bruker RFS 100 FT Raman spectrometer with the resolution of 4 cm^{-1} using 60 scans. Surface acidities of the supported tungsten oxides were determined by microcalorimetry of ammonia adsorption. Before ammonia adsorption, the samples were pre-oxidized at 673 K in oxygen for 1 h, pumped at 673 K for another 2 h, then cooled down to room temperature in vacuum. Calorimetry measurements were performed on a self-assembled differential calorimeter. A very small amount of ammonia was exposed stepwise to saturated adsorption at 423 K.

3. Results and discussion

BET surface areas of the zirconia-supported tungsten oxides as well as of the zirconia support are presented in table 1. Most supported tungsten oxide samples maintain their surface areas compared with the zirconia which was calcination at 773 K. However, after calcination at 973 K, the surface areas of the t-ZrO_2-supported samples decreased dramatically, whether the sample was prepared by supporting tungsten species onto tetragonal ZrO_2 or directly onto the hydroxide precursor of tetragonal ZrO_2. This decrease in surface area is most probably due to the alteration in the texture property at high temperature (973 K) caused originally by the strong base treatment.

Figure 1 shows the XRD patterns of various zirconium oxides prepared via three different preparation procedures. It is clear that both the starting material and the operating conditions have considerable effects on the crystal form of the calcined ZrO_2 sample. In general, the zirconium hydroxide gel was transformed into monoclinic-type ZrO_2 during calcination. On the other hand, the zirconium hydroxide gel obtained by combination of slow addition of concentrated aqueous ammonia and the following treatment with concentrated NaOH solution was converted into

Table 1
The BET surface areas of the zirconia support and zirconia-supported tungsten oxides.

Catalyst	WpmZr	WptZr	WpcZr	WmZr	WtZr	WcZr	ZrO_2
Surface areas (m^2/g)	73	19	53	40	29	60	57–60

Note: The zirconia with a surface area of 57–60 m^2/g was calcined at 773 K. W in the catalyst signs represents tungsten oxides, Zr denotes zirconium oxide, p means prepared by the zirconium hydroxide precursor, m, t and c represent the monoclinic, tetragonal and cubic zirconium oxide, respectively.

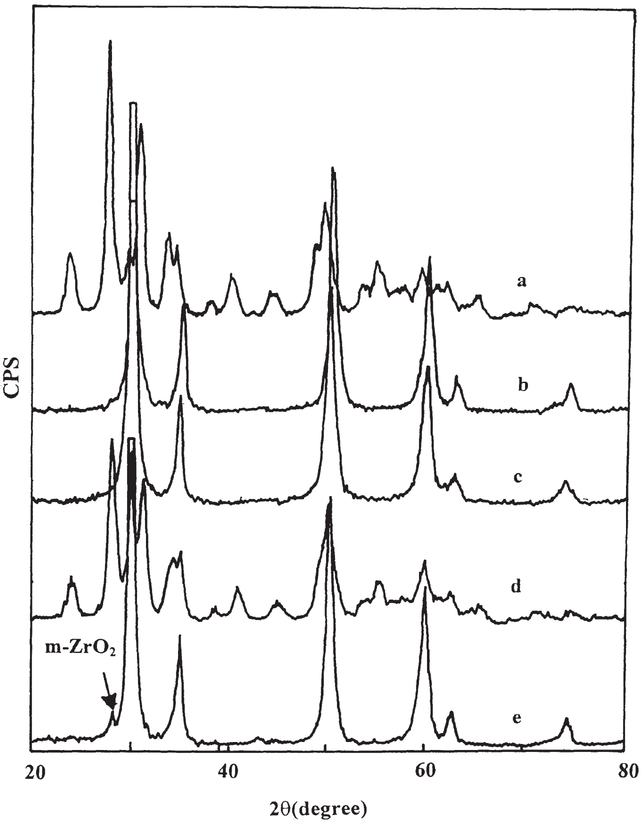

Figure 1. The XRD patterns of various zirconium oxides prepared by different ways. (a) Prepared with $ZrCl_4$, (b) prepared with $ZrCl_4$, the suspension was treated with 4.5 M NaOH solution, (c) prepared with $ZrCl_4$ and $Y(NO_3)_3$, (d) prepared with $ZrOCl_2$, (e) same as (b), but the concentration of NaOH solution is 3.0 M.

tetragonal ZrO_2. If a low concentration of aqueous NaOH was used (3 M), the monoclinic ZrO_2 was already present (as can be seen in figure 1(e)), therefore, the NaOH treatment seems to be a more critical parameter for obtaining the single phase of tetragonal ZrO_2. Slow addition of ammonia and thereafter treatment of the precipitate by a concentrated NaOH solution in particular will lead to altering the nature of the zirconium hydroxide and forming the compact and fine gel particles of zirconium hydroxide, which, in turn, leads to the transformation of zirconium hydroxide into tetragonal ZrO_2 during the calcination procedure. For the well-defined tetragonal ZrO_2 phase, a well-splitting at $2\theta = 32$–$34°$ can be observed in the XRD pattern, but it is absent in our case. As a matter of fact, since, in our case, the hydroxide precursors were calcined only at low temperature, the crystallinity of ZrO_2 was expectantly not so good as that of ZrO_2 obtained by calcining at much higher temperature [12,13]. According to the literature [10], modification of zirconium hydroxide with proper amount of Y component is able to yield cubic ZrO_2. However, it is not easy to distinguish between tetragonal and cubic ZrO_2 by conventional X-ray diffraction. The shift of a small peak at $2\theta \approx 74°$ could be another fingerprint to identify these two types of ZrO_2. Accordingly, with increasing the content of Y_2O_3, the feature of ZrO_2 becomes predominantly cubic. It can also be found in figure 1 that, if $ZrOCl_2$ was used instead of $ZrCl_4$, the final ZrO_2 sample was in an mixed crystal form, namely the monoclinic form of ZrO_2 plus much more amount of tetragonal ZrO_2 (the major peak for the tetragonal phase becomes very intensive, as seen in figure 1(d)). However, if the sample was prepared by $ZrCl_4$ (see figure 1(a)), only a very small amount of tetragonal ZrO_2 was present. This observation revealed that the starting material plays a role in determining the nature of zirconium hydroxide. Such effect has also been studied by Srinivasan and Davis [8]. This is probably due to a different density of anion species as well as different pH in the initial salt solution.

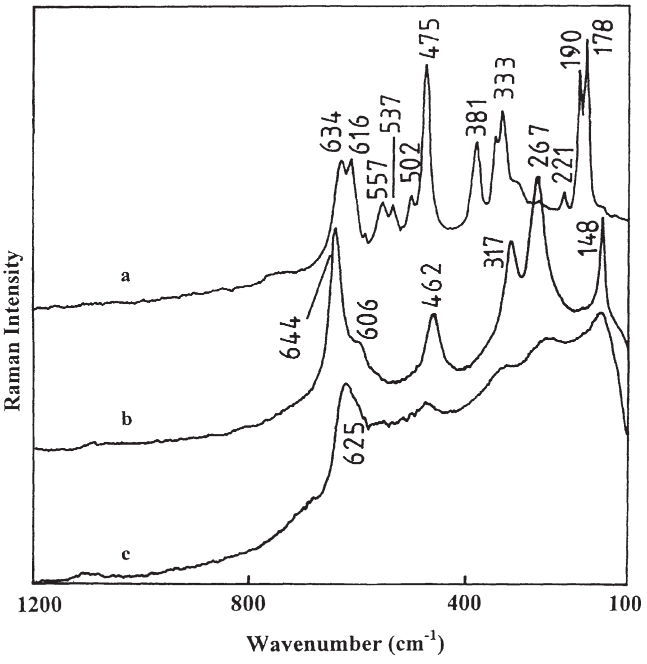

Figure 2. Raman spectra of the zirconium oxides prepared by three different procedures. The results indicated that (a), (b) and (c) are monoclinic, tetragonal and predominantly cubic ZrO_2, respectively.

Our Raman results show more clearly spectroscopic differences between these two types of ZrO_2, as shown in figure 2. For the Y-doped sample, only one intensive peak around 610 cm^{-1} can be found and no other appreciably intensive bands appeared in the 100–700 cm^{-1} range, while for the NaOH-treated sample, there are five intensive peaks present in the same range, which are the characteristics of the tetragonal ZrO_2 [13,14]. In other words, the Y-doped ZrO_2 with 6 mol% Y_2O_3 is in predominantly cubic form.

The XRD patterns of the supported tungsten oxides prepared by originally impregnating zirconium hydroxide precursors are shown in figure 3(a). In general, ZrO_2 and, in some cases, WO_3 crystallites can be distinguished from the samples. The crystal form of ZrO_2 in the WpmZr and WptZr samples is basically the same, namely the tetragonal phase. In the Y-doped sample, WpcZr, ZrO_2 was present as a cubic-like phase. It is worthy to note that there is crystalline WO_3 existing in the WpmZr and WptZr samples, while no WO_3 phase is present in the WpcZr sample. Moreover, the WptZr sample contains much more amount of WO_3 phase as compared with the WpmZr sample. It is also interesting that the $Zr(WO_4)_2$ phase has not been found in the samples, even if there is an extra WO_3 phase present. The observations revealed that the interaction between tungsten species and different kind of ZrO_2 is distinct and controls the forms of tungsten species and their relative content on the support.

When the samples were prepared by impregnating different types of ZrO_2 support, the present tungsten species has less effect on the form of ZrO_2 after calcination, as seen in figure 3(b). The WmZr and WtZr samples maintain the original form of ZrO_2 support, namely the monoclinic and tetragonal, respectively, and contain bulk phase of WO_3. Compared with the WptZr as well as WmZr sample, the WtZr sample has less amount of WO_3 phase. Furthermore, no WO_3 bulk phase was found in the WcZr sample, and, again, the $Zr(WO_4)_2$ phase has not been detected in all three ZrO_2-supported samples by XRD.

The above results lead to the conclusion that the supported tungsten species are able to promote transformation of zirconium hydroxide precursor obtained by different procedures into the certain type of ZrO_2, namely the tetragonal ZrO_2, and to stabilize this state, while it was generally difficult to alter the form of ZrO_2 if an oxide support was initially used instead of hydroxide precursor.

Figure 4(a) shows the Raman spectra of the impregnated ammonium tungstate on the hydroxide precursors before calcination. Apparently, the spectroscopic features of the three samples are almost the same, indicating that the surface states of the tungstate species on the different hydroxide precursors are similar. The main bands at

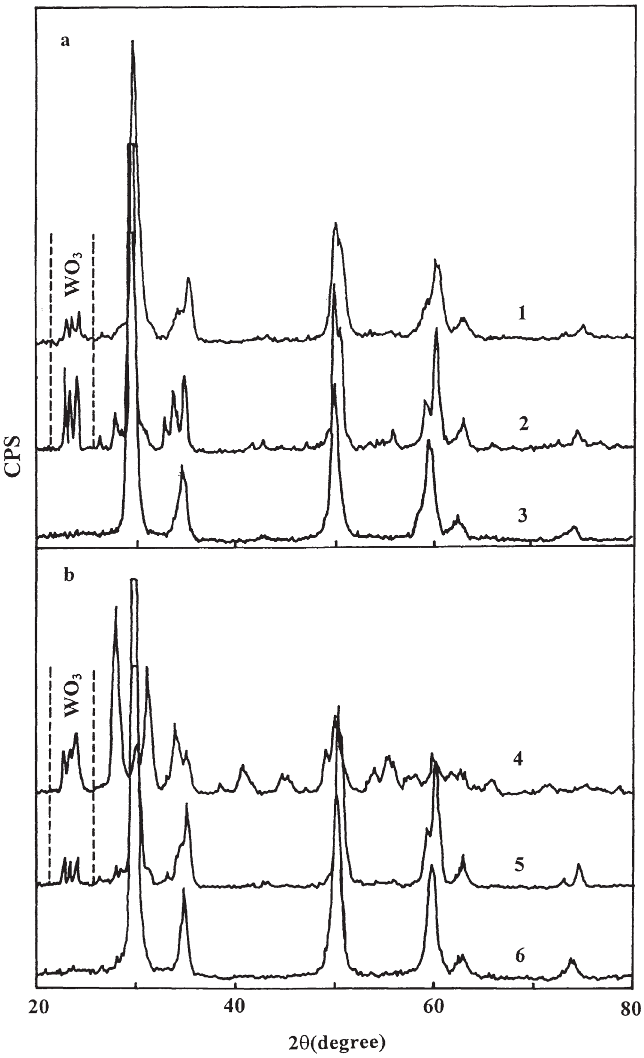

Figure 3. The XRD patterns of the calcined samples prepared by impregnating (a) three zirconium hydroxide precursors and (b) three types of zirconium oxides with ammonium tungstate(VI). (1) WpmZr, (2) WptZr, (3) WpcZr, (4) WmZr, (5) WtZr, (6) WcZr.

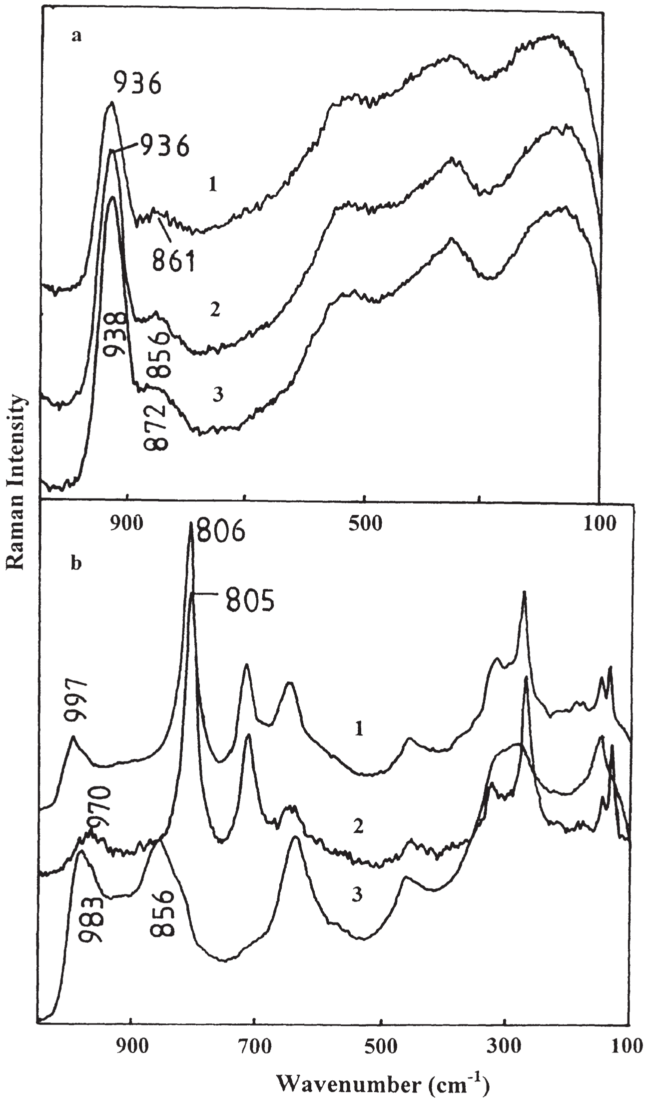

Figure 4. Raman spectra of three tungstate-containing zirconium hydroxide precursors. (a) Before and (b) after calcination. (1) WpmZr, (2) WptZr, (3) WpcZr.

$\sim$353, 860 and 935 cm^{-1} are due to the vibration modes of ν_b, ν_{as} and ν_s of the W=O group in the surface tungstate species, respectively. After calcination of these three impregnated precursors, as shown in figure 4(b), two things occurred: (1) For the WpmZr and WptZr samples, the Raman features are very similar to each other, except the band at $\sim$980 cm^{-1}. This band was red-shifted for the latter sample, implying that the interaction between the surface tungsten species and ZrO_2 is relatively stronger. Besides the surface two-dimensional tungsten oxide species (970–997 cm^{-1}), there is crystalline WO_3 existing in both samples, corresponding to the Raman bands at 804, 713 and 273 cm^{-1} (the last band was partly overlapped with the band of ZrO_2). All these observations are in good agreement with the XRD results. (2) Very different Raman features can be observed on the WpcZr sample, and moreover, only one kind of tungsten species can be monitored, that is, the two-dimensional tungsten oxide overlayers. It also revealed that another type of surface tungsten oxide species, likely the precursor of crystalline WO_3, was present in this sample, corresponding to the band at 856 cm^{-1}. The band positions as well as intensities of the vibration of the W–O bond changed notably after calcination, indicating that the nature of surface tungsten species was altered obviously by the high-temperature treatment.

For the dried samples obtained by directly impregnating ZrO_2, seen in figure 5(a), the band features due to surface tungstate species again are quite similar among the three samples. If compared with those of hydroxide-supported precursors, we can conclude that the surface states of tungstates on both ZrO_2 and $ZrO_2{\cdot}x H_2O$ are indeed not so much distinct. One apparent difference is that the major band is shifted somewhat toward the high wavenumber end. On the other hand, the bands in the 100–700 cm^{-1} range are significantly different from one sample to another. They are the characteristics of monoclinic, tetragonal and predominantly cubic ZrO_2, respectively. When calcined, as

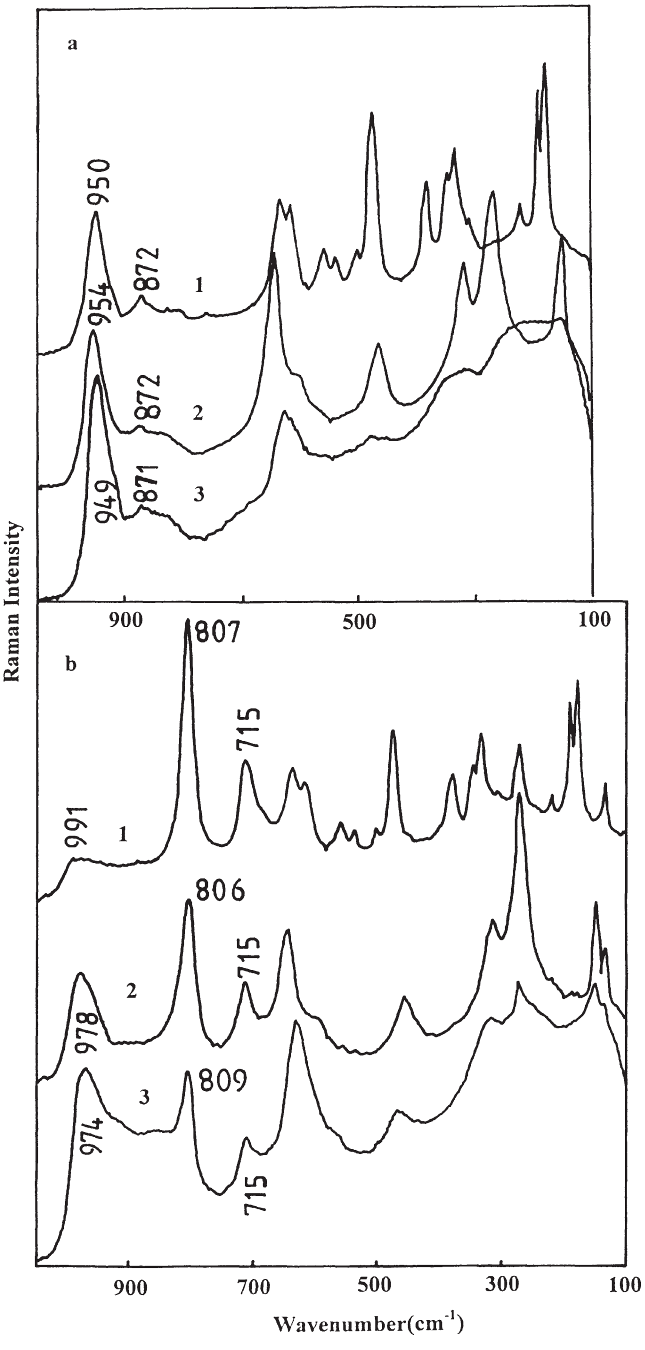

Figure 5. Raman spectra of different zirconium oxides impregnated with ammonium tungstate(VI). (a) Before and (b) after calcination. (1) WmZr, (2) WtZr, (3) WcZr.

shown in figure 5(b), two kinds of tungsten species were figured out in all three samples. This is different from what can be observed in figure 4(b). In addition to the crystalline WO_3, similar features of the surface tungsten species can be seen except a slight band shift of the W–O bond vibration. It should be noted that the ratio of surface tungsten oxide species to WO_3 bulk phase changed greatly from the WmZr to the WcZr sample. In the first sample, the major tungsten component is the bulk phase of WO_3, while in the last sample, the major component is the surface tungsten oxide overlayers. As already observed in the WpcZr sample, another type of surface tungsten oxide species with the band at ~855 cm^{-1} (this band is overlapped with the bands at 974 and 715 cm^{-1}) may also be present in the WcZr sample, although the content is relatively low. Moreover, WO_3 bulk phase is not examinable in the WcZr by XRD, but can be clearly distinguished by Raman spectroscopy. It is to be pointed out that one band at 635 cm^{-1} becomes very intensive after calcination in the WpcZr and WcZr samples. This band is likely due to the vibration in the W–O–W group and may be the indication of a higher degree of bridge-links of surface WO_x ensembles. For the WcZr sample, it can also be found that the crystal feature of ZrO_2 tunes to be some tetragonal character after calcination, and this is very difficult to be revealed by the XRD technique.

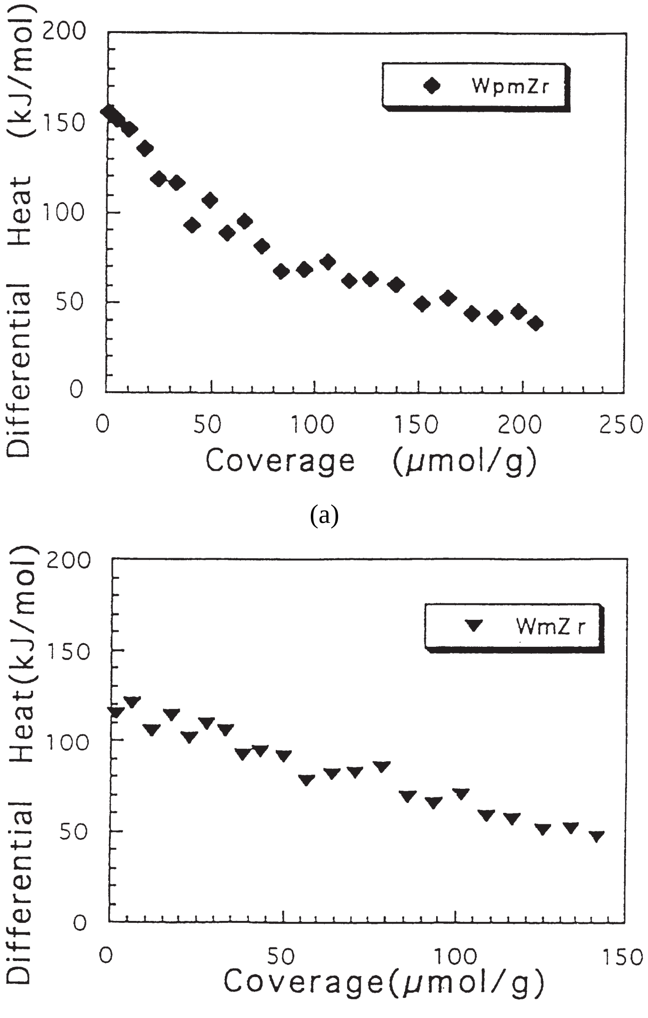

(a)

(b)

Figure 6. Microcalorimetry results of ammonia adsorption on the zirconia-supported tungsten oxides. (a) WpmZr, (b) WmZr.

The surface acidities of these tungsten-containing samples were measured by Tian–Calvet-type microcalorimetry using ammonia as a basic probe molecule. The results are shown in figures 6–8. Although the catalytic data have not been collected yet to give additional correlation between the catalytic performance and the surface acidity, the calorimetric results already provided a criterion for paral-

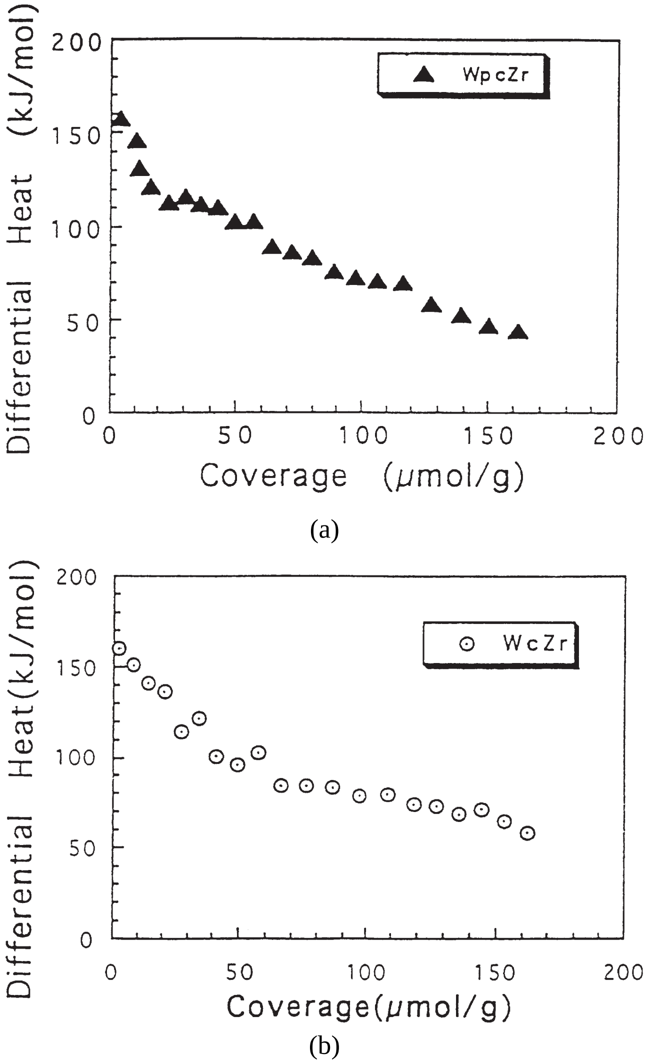

(a)

(b)

Figure 7. Microcalorimetry results of ammonia adsorption on the zirconia-supported tungsten oxides. (a) WpcZr, (b) WcZr.

lel comparing the surface acidity among the samples. For the WpmZr, WpcZr and WcZr samples, the differentially initial adsorption heat is quite large (155–160 kJ/mol), indicating the presence of very strong acidic sites. According to the studies of Nakano et al. [15], Shibata et al. [16] and Chan et al. [17], ZrO_2 itself only shows weakly acidic property. Therefore, the generation of strong acidic sites should be correlated with the cooperation of tungsten species and ZrO_2. Since the crystal form of ZrO_2 in these samples is tetragonal or cubic, the creation of the strong surface acidity is closely related to the structure of the tetragonal or cubic phase. As a matter of fact, the structural feature of tetragonal and cubic is principally similar, in other words, the structure of the tetragonal phase can be regarded as that of the cubic phase with the certain distortion. For this reason, it is not difficult to understand why the strong acidic sites can also be created on the predominantly cubic phase. It is also suggested that generation of the strong acidic sites due to cooperation of tungsten species and ZrO_2 is not sensitive to the degree of distortion from cubic to tetragonal structure, but is very sensitive to the structural difference between monoclinic and tetragonal or cubic phase. This is clearly demonstrated by the case of the WmZr sample, in which ZrO_2 is in monoclinic form. On the other hand, the surface acidic properties were not influenced by introducing the yttrium component, as observed over the yttrium-containing samples. It is very surprising to find that the initial adsorption heat on either the WptZr or the WtZr sample is quite small, indicating that the strong acidic centers have not been generated. Since the crystal form of ZrO_2 is tetragonal in both samples and the structural features of the tungsten species are also similar to those of the samples with the strong acidic sites, there must be some other reason for this unexpected observation. Because the zirconium hydroxide had been treated with concentrated NaOH solution, it is speculated that there might be some sodium ions remaining in the NaOH-treated samples. This assumption was confirmed by ICP and XPS investigations. ICP results indicated that only a trace of sodium ions is present in the bulk phase of samples (b) and (e) through extensive washing. XPS results revealed, however, the surface concentration

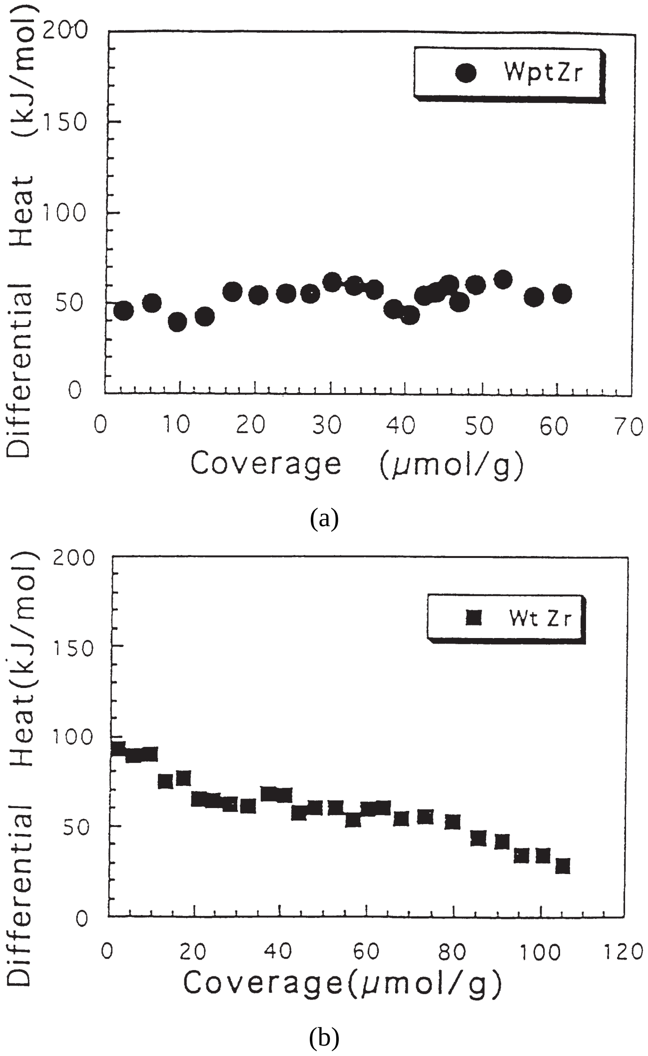

(a)

(b)

Figure 8. Microcalorimetry results of ammonia adsorption on the zirconia-supported tungsten oxides. (a) WptZr, (b) WtZr.

of sodium ions is approximately 4–5% determined using the peak area sensitivity factor, suggesting the segregation of sodium ions on the sample surface. Very likely, these surface sodium ions can prohibit the generation of strong acidic sites or poison these sites. Although no crystalline WO_3 phase exists in the WpcZr sample, it still exhibits very large initial adsorption heat, suggesting that the strong acidic centers should be principally and closely related to the two-dimensional tungsten oxide specimen with the Raman bands in the 974–997 cm^{-1} range. In summary, the samples WpmZr, WpcZr and WcZr, which show similar high calorimetric heats of NH_3 adsorption, all contain the essential two-dimensional tungsten oxides, with the corresponding Raman bands at 997, 983 and 974 cm^{-1} and the essential tetragonal (cubic) ZrO_2 phase. Other present tungsten oxide species, namely crystalline WO_3 or the precursor of crystalline WO_3 or their combination, with the Raman bands in the 600–900 cm^{-1} range, are not important for building up strong acidic strength.

4. Concluding remarks

Three different types of ZrO_2 and their hydroxide precursors were prepared in a controllable way. The starting material and the different preparing conditions are able to affect considerably the final ZrO_2 structure. The zirconium-hydroxide-supported tungsten species will promote the transformation of different kinds of hydroxides into tetragonal ZrO_2. Such effect, however, is difficult to occur on the ZrO_2-supported systems. The structures of impregnated surface tungstates on three zirconium hydroxide precursors or three types of zirconia are similar. Before calcination, the structural differences in the surface tungstates between hydroxide-precursor- and oxide-supported samples are insignificant. After heat treatment, however, considerable alterations occurred in the structures of tungsten species on the two series samples. The tungsten components in the calcined samples are the surface tungsten oxides together with the crystalline WO_3. The ratio of the two species is affected by the preparation history and the nature of support. Generation of strong acidic sites will be dependent on the crystal structure of ZrO_2 phase, the type of tungsten oxide species and the cooperation between the surface tungsten oxide overlayer and ZrO_2. Remaining sodium ion impurities can prohibit creation of strong acidic sites or directly poison these sites, introduction of an yttrium component into zirconium oxide, however, has not shown appreciable effect on the surface acidity.

References

[1] K. Tanabe, H. Hattori, T. Yamaguchi and T. Tanaka, eds., *Acid–Base Catalysis* (Kadansha, Tokyo, 1989).

[2] K. Tanabe, M. Misono, Y. Ono and H. Hattori, *New Solid Acids and Bases* (*Their Catalytic Properties*), Stud. Surf. Sci. Catal., Vol. 51 (Kodansha, Tokyo, 1989).

[3] M. Hino and K. Arata, J. Chem. Soc. Chem. Commun. (1979) 1148.

[4] M. Hino and K. Arata, J. Chem. Soc. Chem. Commun. (1980) 851.

[5] M. Hino and K. Arata, J. Chem. Soc. Chem. Commun. (1987) 1259.

[6] M. Hino and K. Arata, Chem. Lett. (1989) 971.

[7] R. Srinivasan, M.B. Harris, S.F. Simpson, R.J. Deangelis and B.H. Davis, J. Mater. Res. 3 (1988) 787.

[8] R. Srinivasan and B.H. Davis, Catal. Lett. 14 (1992) 165.

[9] S. Sugiyama, K. Shimodan, H. Hayashi, N. Shigemoto, K. Miyaura, K. Saitoh and J.B. Moffat, J. Catal. 141 (1993) 279.

[10] M.K. Dongare and A.P.B. Sinha, J. Mater. Sci. 19 (1984) 49.

[11] K. Arata, Adv. Catal. 37 (1989) 165.

[12] G. Fagherazzi, P. Canton, A. Benedetti, F. Pinna, G. Mariotto and E. Zanghellini, J. Mater. Res. 12 (1997) 318.

[13] T. Hirata, E. Asari and M. Kitajima, J. Solid State Chem. 110 (1994) 201.

[14] J.G. Cai, Y.S. Raptis and E. Anastassakis, Appl. Phys. Lett. 62 (1993) 2781.

[15] Y. Nakano, T. Iizuka, H. Hattori and K. Tanabe, J. Catal. 57 (1978) 1.

[16] K. Shibata, T. Kiyoura, J. Kitagawa, T. Sumiyoshi and K. Tanabe, Bull. Chem. Soc. Jpn. 46 (1973) 2985.

[17] K.S. Chan, G.K. Chuan and S. Jaenicke, J. Mater. Sci. Lett. 13 (1994) 1579.